4. Li X, Zhao Q, Wu K, Fan D. I148M variant of PNPLA3 confer increased risk for nonalcoholic fatty liver disease not only in European population, but also in Chinese population. HEPATOLOGY 2011; doi: 10.1002/hep.24567.
5. Zeng MD, Fan JG, Lu LG, Li YM, Chen CW, Wang BY, et al. Guidelines for the diagnosis and treatment of nonalcoholic fatty liver diseases. J Dig Dis 2008;9:108-112.

View this article online at wileyonlinelibrary.com.
DOI 10.1002/hep.24659
Financial support provided by National Institutes of Health grants RL1HL092550 and RO1DK090066.
Potential conflict of interest: Dr. Hobbs consults for Pfizer.

Staging Hepatic Fibrosis: Computer-Aided Analysis of Hepatic Contours on Gadolinium Ethoxybenzyl Diethylenetriaminepentaacetic Acid-Enhanced Hepatocyte-Phase Magnetic Resonance Imaging

To the Editor:

Chronic liver diseases can lead to hepatic fibrosis, cirrhosis, the development of hepatocellular carcinoma, and contribute substantially to healthcare costs.[1] Detection and grading of hepatic fibrosis currently requires a biopsy, which subjects the patient to a risk of serious complications.[2] Liver surface nodularity reflects the presence of regenerative nodules and fibrous septa, which are the essential histologic findings for the diagnosis of cirrhosis.[3,4] Gadolinium ethoxybenzyl diethylenetriaminepentaacetic acid (Gd-EOB-DTPA) is a liver-specific magnetic resonance imaging (MRI) contrast medium and its hepatocyte-phase images yield excellent hepatic

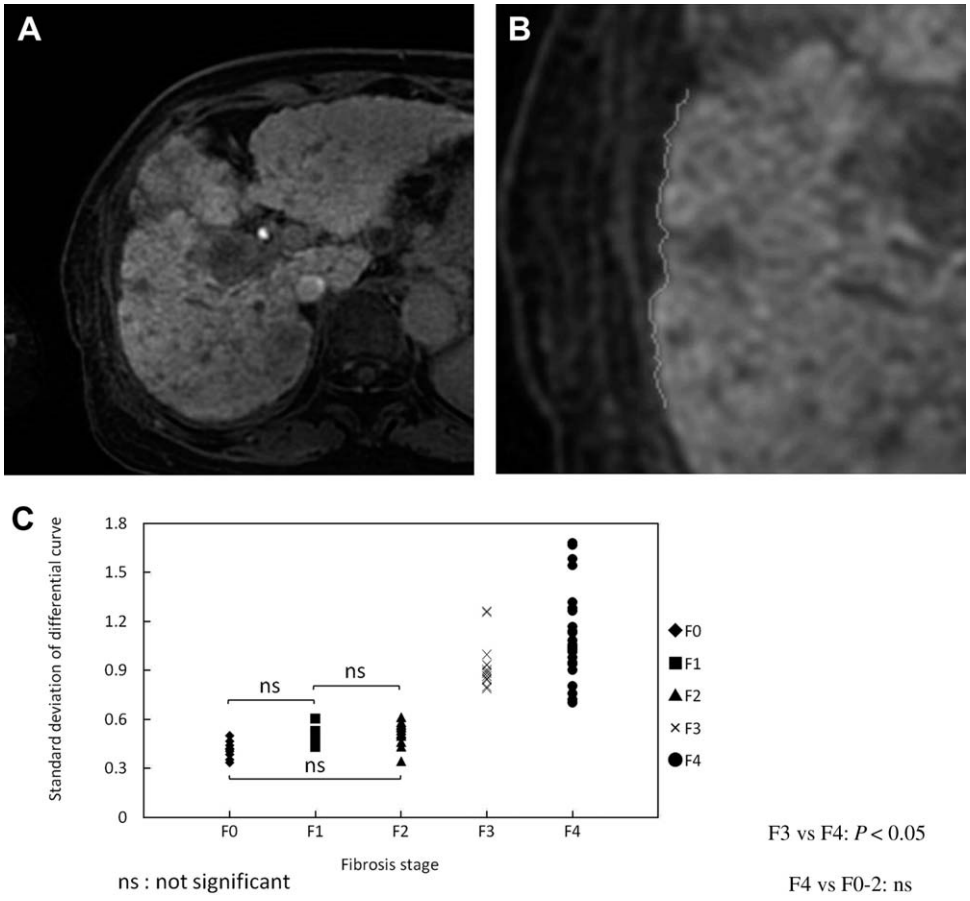

Fig. 1. A 73-year-old woman with fibrosis stage F4 due to hepatitis C virus. Axial T1-weighted image (fat-suppressed three-dimensional spoiled fast field-echo [TR/TE, 4.0/1.9 ms]; field-of-view, 42 × 29 cm; 336 × 168 image matrix [512 × 512 reconstruction]; parallel imaging factor, 1; flip angle, 13°; slice thickness, 4.4-mm section thickness with 2.2-mm overlap; acquisition time, 90 slices per each phase during 22-second breath holding) at the hepatic hilar level obtained in the hepatocyte phase (A) was magnified twice to trace the hepatic surface profile (B). More than 128 points with quarter pixel size were requested in this stage. Hepatic profile curve ($f_{(x)}$) was obtained by making a straight line between the start and endpoint of the hepatic profile obtained in (B), then rotating parallel to the x-axis. An approximate curve ($D_{(x)}$) was determined by a least-square approach with an n-th degree polynomial equation which produced the highest R^2 value. An approximate curve ($D_{(x)}$) in this case was expressed by a twenty-ninth degree polynomial equation with R^2 value of 0.788. The difference between $D_{(x)}$ and $f_{(x)}$ was calculated ($S_{(x)} = D_{(x)} - f_{(x)}$) and then a standard deviation of $S_{(x)}$ (SD) was used for possible MRI parameters. (C) Mean ± SD was higher in patients with F4 than with F3 ($P < 0.05$), whereas they still overlapped. No significant difference was found between F0, F1, and F2. ns, not significant.

enhancement and the objective delineation of hepatic contour morphology. We thus conducted a computer-aided diagnosis algorithm based on the hepatic contour morphological features such as surface nodularity for predicting hepatic fibrosis stages.

Between February 2010 and January 2011, 87 patients (56 male, 31 female; age range, 39-85 years, hepatitis C in 72, hepatitis B in 12, alcohol abuse in 2, and cryptogenic in 1) with pathologically proven hepatic fibrosis stages underwent Gd-EOB-DTPA-enhanced MRI with a 3T superconducting system. Stage was determined by: hepatectomy (n = 32) to treat hepatic tumors or percutaneous liver biopsy (n = 55). Fibrosis stages were determined according to the established criteria[5]: F0 (n = 9); F1 (n = 16); F2 (n = 13); F3 (n = 21); and F4 (n = 28).

According to our algorithm (Fig. 1), the mean ± SD was significantly higher in patients with ≥F3 than with ≤F2 ($P < 0.001$, Tukey criterion). No significant difference was found among F0, F1, and F2. Although the mean ± SD of F4 was higher than that of F3 ($P < 0.05$), there was a considerable overlap in their distribution. Post-hoc power analysis showed that we had 80.9% power to detect a 15% difference in linear multiple regression analysis between fibrosis stages. Both the sensitivity and specificity of SD for the diagnosis of hepatic fibrosis stages ≥F3 were 100% using a cutoff value of 0.65 (Fig. 1c).

We have successfully applied a computer-aided analysis of hepatic contour that was highly accurate in diagnosing hepatic fibrosis stages F3 and F4 and may be a useful imaging biomarker for staging hepatic fibrosis.

Acknowledgment: Supported in part by the Health and Labour Sciences Research Grants for Third Term Comprehensive Control Research for Cancer.

Satoshi Goshima, M.D.[1]
Masayuki Kanematsu, M.D.[1]
Tatsunori Kobayashi, R.T., M.S.[2]
Takahiro Furukawa, B.S.[2]
Xuejun Zhang, Ph.D.[2]
Hiroshi Fujita, Ph.D.[2]
Haruo Watanabe, M.D.[1]
Hiroshi Kondo, M.D.[1]
Noriyuki Moriyama, M.D.[3]
Kyongtae T. Bae, M.D, Ph.D.[4]

[1]*Department of Radiology*
Gifu University Hospital
Gifu, Japan
[2]*Department of Intelligent Image Information*
Division of Regeneration and Advanced Medical Sciences
Graduate School of Medicine
Gifu University, Gifu, Japan
[3]*Department of Diagnostic Radiology*
National Cancer Center Hospital
Tokyo, Japan
[4]*Department of Radiology*
University of Pittsburgh Medical Center
Pittsburgh, Pennsylvania, USA

References

1. Afdhal NH, Nunes D. Evaluation of liver fibrosis: a concise review. Am J Gastroenterol 2004;99:1160-1174.
2. Piccinino F SE, Pasquale G, Giusti G. Complications following percutaneous liver biopsy: a multicentre retrospective study on 68,276 biopsies. J Hepatol 1986;2:165-173.
3. Colli A, Fraquelli M, Andreoletti M, Marino B, Zuccoli E, Conte D. Severe liver fibrosis or cirrhosis: accuracy of US for detection—analysis of 300 cases. Radiology 2003;227:89-94.
4. Schalm SW. The diagnosis of cirrhosis: clinical relevance and methodology. J Hepatol 1997;27:1118-1119.
5. Ichida F, Tsuji T, Omata M, Ichida T, Inoue K, Kamimura T, et al. New Inuyama classification; new criteria for histological assessment of chronic hepatitis. Int Hepatol Commun 1996;6:112-119.

View this article online at wileyonlinelibrary.com.
DOI 10.1002/hep.24677
Potential conflict of interest: Nothing to report.

Acute Fulminant Hepatitis with Bone Marrow Failure in an Adult Due to Parvovirus B19 Infection

To the Editor:

Infection by parvovirus B19 is widespread and can be associated with a wide range of different pathologies and clinical manifestations.[1] It mainly causes the childhood exanthema erythema infectiosum and an influenza-like condition with polyarthropathy.[2] In rare cases, parvovirus B19 infection has been associated with hepatic dysfunction and hematologic disease in adult.[3,4] We describe here a case of acute fulminant hepatitis with bone marrow failure in a healthy adult following asymptomatic infection with B19 virus.

A previously healthy 34-year-old woman without history of previous liver disease, exposure to toxic agents, or alcohol abuse reported to our practice after 20 days of fever; a week of yellowish staining of sclera, skin, and urine; and wrist and ankle joint pain on both sides (Table 1, day 1). She was hospitalized and given oral doses of prednisone and ibuprofen in addition to 5 days of intravenous infusion of penicillin and erythromycin. Her joint pain decreased, but the fever remained, the highest body temperature being 107.6°F. After maculopapules appeared on her back with significant pruritus (Figure 1) and her laboratory results worsened (Table 1, day 7), she was transferred to our facility. Physical examination revealed jaundice, fever, and hepatomegaly. Rheumatoid factor, alpha-1-antitrypsin level, antinuclear antibody, double-stranded DNA antibody, liver-kidney microsomal type 1 antibody, smooth muscle actin antibody, blood culture, and tuberculin tests were unrevealing. Abdominal ultrasound revealed only homogeneous enlargement of the liver and spleen, and chest radiographs and abdominal computed tomography scans were noncontributory. Serology was negative for hepatitis A, B, C, D, E, or G virus; cytomegalovirus; Epstein–Barr virus;